Measurement, Simulation, and Theory of a Non-Foster Unit Cell with Parasitic Resistance

Kathryn L. Smith, Thomas P. Weldon, and Ryan S. Adams
Department of Electrical and Computer Engineering
University of North Carolina at Charlotte
Charlotte, N.C., USA

***Abstract*—Measured, simulated, and theoretical results are presented for a metamaterial unit cell loaded by a non-Foster circuit element comprising a negative capacitor. The unit cell is suspended in the electromagnetic field of a coaxial line for characterization, rather than being directly wired to the transmission line. Relative dielectric constant less than unity was observed over a 5:1 bandwidth, and supporting theory is presented showing that bandwidth can be improved by reducing parasitic resistance of the non-Foster element. Simulated, measured, and theoretical results that show similar bandwidth and permittivity characteristics.**

I. Introduction

Non-Foster circuits are being investigated for applications in wideband metamaterials, artificial magnetic conductors, and wideband antenna matching. A number of investigators have presented metamaterials loaded with non-Foster circuits directly wired into waveguide and transmission line sections [1], [2]. The present paper considers non-Foster loaded CLS (capacitively loaded strip) unit cells suspended in a coaxial line section, excited by the electromagnetic field without being directly wired to the coaxial line [3]. As noted by other investigators, component parasitics and quality factor (Q) impact performance and bandwidth of non-Foster applications [2]. Therefore, such parasitic effects are included in present work, resulting in simulated, measured, and theoretical results showing similar bandwidth and permittivity characteristics.

II. Theory

The metamaterial unit cell under consideration consists of an "I"-shaped CLS (capacitively loaded strip) [3] suspended in a coaxial line, as shown in Fig. 1. In the absence of non-Foster loading, the CLS unit cell may be modeled as a very small electric dipole with capacitance C_d and length l_d loaded with inductance L_d, in an effective volume V_d, with narrowband negative electric susceptibility [3]

$$\chi_e = \frac{l_d^2/\left(\epsilon_\circ V_d\right)}{j\omega\left(j\omega L_d + 1/\left(j\omega C_d\right)\right)} = \frac{\left(C_d l_d^2\right)/\left(\epsilon_\circ V_d\right)}{1-\omega^2 L_d C_d}\,, \qquad (1)$$

where $\epsilon_\circ = 8.85\times10^{-12}$ F/m is the permittivity of free space. By replacing the inductive post in the CLS with capacitance C_p having both a series parasitic resistance R_s and a parallel parasitic resistance R_p, the result of (1) becomes

$$\chi_e = \frac{l_d^2 C_d\left(s\left(R_s+R_p\right)C_p+1\right)/\left(\epsilon_\circ V_d\right)}{s^2 R_s R_p C_d C_p + s\left(R_p(C_p+C_d)+R_s C_p\right)+1}\,. \qquad (2)$$

For $R_p = \infty$ and $R_s = 0$ the result in (2) becomes independent of frequency at low frequencies and can be approximated as

$$\chi_e \approx \frac{l_d^2}{\epsilon_\circ V_d}\,\frac{C_p C_d}{C_p + C_d}\,, \qquad (3)$$

where (3) has the same wideband form as the result in [4] for a similar unit cell: $\chi_e = \left[l_p/\left(\epsilon_\circ l_x l_z\right)\right]\left(C_0\, C_p\right)/\left(C_p + C_F\right)$. Note that χ_e can become a relatively large negative value when $C_p < 0$, and $C_p + C_d > 0$, and $|C_p + C_d| << C_d$.

Comparing (2) and (3), the theoretical effective electric susceptibility χ_e and effective relative permittivity $\epsilon_r = 1+\chi_e$ of the non-Foster loaded CLS unit cell is bandlimited by the parasitic resistances R_p and R_s that lead to the quadratic in the denominator of (2). From (2), the theoretical value of $\epsilon = 1 + \chi_e$ for the case where $R_s = -133\,\Omega$, $R_p = 220\,k\Omega$, $C_d = 2.5$ pF, $C_p = -2.4$ pF, $l_d = 0.02$ m, $V_d = 1.21\times10^{-3}$ m^3 is shown in t Fig. 2.

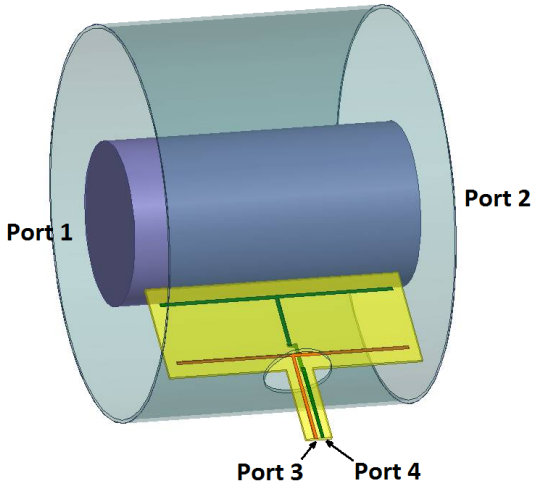

Fig. 1. The CLS metamaterial unit cell in a coaxial line section. The CLS consists of 1 mm copper traces on a $76.2 \times 32 \times 0.79$ mm FR4 substrate. The inner conductor of the coaxial line has a diameter of 24 mm, and the outer conductor has a diameter of 115 mm. The outer conductor is supported by a 1 mm thick pipe of ABS plastic. Two traces protrude through a hole in the coax shield, providing access to the metamaterial from outside.

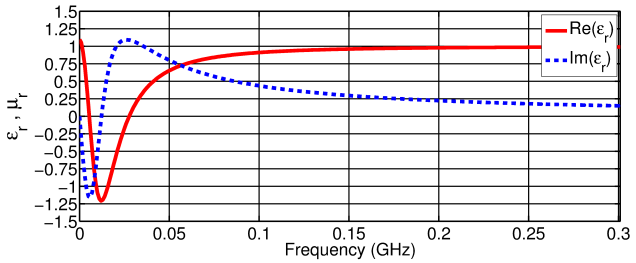

Fig. 2. Theoretical relative permittivity $\epsilon_r = 1 + \chi_e$ using (2), with parasitics $R_s = -133\,\Omega$, $R_p = 220\,k\Omega$, dipole capacitance $C_d = 2.5$ pF, non-Foster load capacitance $C_p = -2.4$ pF, $l_d = 0.02$ m, and$V_d = 1.21 \times 10^{-3}$ m^3. Real (solid red) and imaginary (dotted blue) parts of theoretical relative permittivity for $\epsilon_r = 1 + \chi_e$. (

III. Simulation And Measured Results

The metamaterial unit cell in the coaxial line section was simulated in Ansys HFSS software, with lumped ports defined at either end of the coaxial line, and also at the ends of each of the two traces that protrude through the coax shield, as shown in Fig. 1. A Linvill negative capacitor, shown in 3, was designed and simulated in the Keysight ADS simulator, and was shown in simulation to have the C_d, R_s, and R_p values used in the calculations above.

The four-port parameters from the HFSS simulation were imported into ADS, and the negative capacitor was connected between ports 3 and 4, as shown in Fig. 3. The resulting S-parameters between ports 1 and 2 were used with the extraction method presented in [6] to obtain the effective permeability and permittivity values of the metamaterial. These simulation results are shown in Fig. 4 (a).

The measured permittivity and permeability of the metamaterial are presented in Fig. 4 (b). Permittivity is shown to be sub-unity from 5 MHz to 25 MHz, corresponding to a 5:1 bandwidth, or 133%. The measured results of Fig. 4(b) show remarkable agreement with the simulation results of Fig. 4(a). Both Fig. 4(a) and Fig. 4(b) show similar bandwidth and

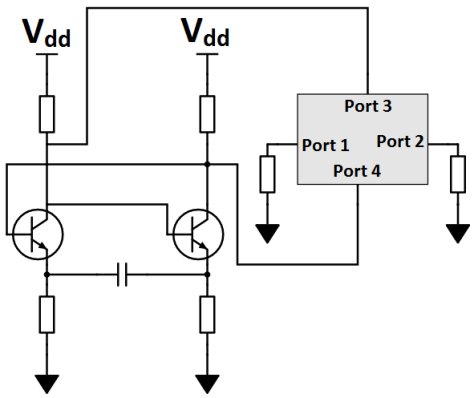

Fig. 3. Schematic for Linvill negative capacitance circuit [5], loaded with metamaterial. The four-port block to the right represents the coaxial line section shown in Fig. 1. As shown, the non-Foster circuit element is connected between ports 3 and 4, corresponding to the protruding traces from the metamaterial.

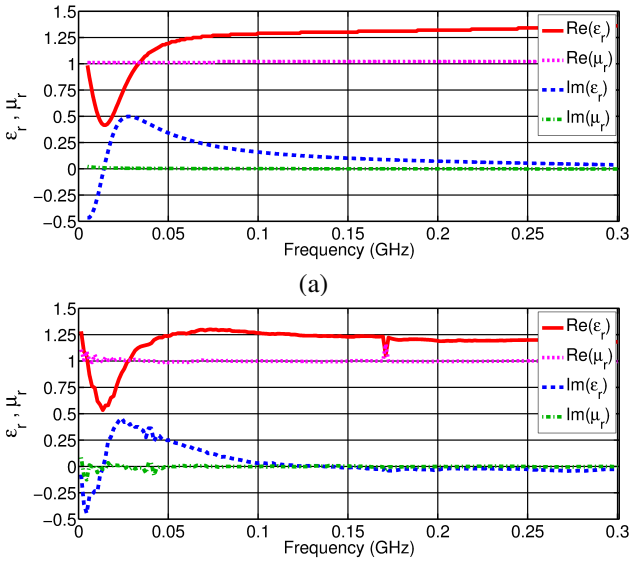

Fig. 4. Simulated and measured results. (a) Transistor-level simulation results from Keysight ADS showing extracted permeability and permittivity for the non-Foster loaded unit cell in the coaxial line using the extraction method in [3], and with 4-port S-parameters of Fig. 1 imported from HFSS simulation. (b) Measured results for a prototype showing extracted permeability and permittivity for the non-Foster loaded unit cell of Fig. 1 using the extraction method in [6], modified so that imaginary parts of μ and ϵ are negative for passive media. In both (a) and (b), the real and imaginary parts of permeability and real and imaginary parts of permittivity are shown in dotted magenta, dot-dashed green, solid red, and dashed blue, respectively.

similar topological behavior over frequency, when compared with the theoretical results of Fig. 2, although there appears to be an offset bias in measured results relative to theory. The elevated high-frequency dielectric constant of $\sim$1.25 in Fig. 4(a) and Fig. 4(b), may suggest a need to include FR4 and ABS loading effects in the theoretical results of Fig. 2 in future investgations.

Acknowledgment

This material is based upon work supported by the National Science Foundation under Grant No. ECCS-1101939.

References

[1] S. Hrabar, I. Krois, I. Bonic, and A. Kiricenko, "Ultra-broadband simultaneous superluminal phase and group velocities in non-Foster epsilon-near-zero metamaterial," *Applied Physics Letters*, vol. 102, no. 5, pp. 054 108–1–5, 2013.

[2] J. Long, M. Jacob, and D. Sievenpiper, "Broadband fast-wave propagation in a non-Foster circuit loaded waveguide," *IEEE Trans. Microw. Theory Tech.*, vol. 62, no. 4, pp. 789–798, Apr. 2014.

[3] R. Ziolkowski, "Design, fabrication, and testing of double negative metamaterials," *IEEE Trans. Antennas Propag.*, vol. 51, no. 7, pp. 1516–1529, Jul. 2003.

[4] T. P. Weldon, K. Miehle, R. S. Adams, and K. Daneshvar, "A wideband microwave double-negative metamaterial with non-Foster loading," in *SoutheastCon, 2012 Proceedings of IEEE*, Mar. 2012, pp. 1–5.

[5] J. Linvill, "Transistor negative-impedance converters," *Proc. of the IRE*, vol. 41, no. 6, pp. 725–729, Jun. 1953.

[6] Z. Szabó and, G.-H. Park, R. Hedge, and E.-P. Li, "A unique extraction of metamaterial parameters based on Kramers-Kronig relationship," *IEEE Trans. Microw. Theory Tech.*, vol. 58, no. 10, pp. 2646–2653, Oct. 2010.